

Deformation Analysis of Brass in Micro Compression Test with Presence of Ultrasonic Vibration

Yang Bai^{1,#} and Ming Yang²

¹ Institute of Forming Technology and Equipment, School of Materials Science and Engineering, Shanghai Jiao Tong University, 1954 Huashan Road, Shanghai, 200030, China

² Graduate School of System Design, Tokyo Metropolitan University, 6-6 Asahigaoka, Hino, Tokyo, 191-0065, Japan

Corresponding Author / E-mail: baiyangsky@sjtu.edu.cn, TEL: +86-21-62833408, FAX: +86-21-62833408

KEYWORDS: Ultrasonic, Softening effect, Compression test, FEM

The application of ultrasonic vibration in metal forming is attracting more attention due to the better performance of ultrasonic-assisted process. By adding small vibration amplitude on tools, the plastic deformation behavior of metal material would differ from the static process. In this study, ultrasonic-assisted compression test was carried out to investigate the influences induced by ultrasonic systematically. Ultrasonic influences on material flow stress, friction and temperature were analyzed. Acoustic softening effect was found size dependent and a new model on basis of surface grain model was proposed to explain it. Numerical simulations were carried out to validate and compare with experimental results.

Manuscript received: July 28, 2014 / Revised: December 28, 2014 / Accepted: January 5, 2015

1. Introduction

Ultrasonic has good directivity and high penetrability, which makes it easy to obtain high concentrated acoustic energy. Since the ultrasonic-assisted metal forming was first proposed in 1955 by Blaha, a considerable amount of relevant research has been done to clarify the mechanism and improve performance. Blaha and Langenecker investigated influence of ultrasonic vibration on metal forming in tensile test.^{1,2} They found that with presence of ultrasonic, the yield stress and flow stress were reduced. This phenomenon is referred as “blaha effect”. Huang³ observed similar phenomenon in his research. By deforming the metal ball, the deformability was found increased with ultrasonic vibration due to the blaha effect of ultrasonic. The blaha effect was linearly proportional to the amplitude of the ultrasonic. The work done by S. Abdul Aziz and M. Lucas⁴ also showed in metal forming test, the forming load was decreased with ultrasonic vibration, and the effect of ultrasonic excitation of the die in metal forming was highly dependent on the material and its capacity to absorb ultrasonic energy and the amplitude of the ultrasonic had a significant effect on the reduction in forming force. Except the reduced flow stress with superimposed vibration, the friction coefficient was also found decreased.⁵ The reduced flow stress in forming process is attributed to the three mechanisms: stress superposition, acoustic softening (blaha effect) and friction decrease,^{6,7} and the acoustic softening is considered

to be the dominating mechanism that leads to the load reduction.

Although ultrasonic vibration has been applied in many metal forming processes, its influences in micro forming is not investigated quantitatively, and the size dependence of ultrasonic vibration effect is not clear. In this study, influences of ultrasonic on material deformation behavior were investigated systematically in ultrasonic vibration-assisted compression (UVAC) test. Material flow stress and friction coefficient were obtained with presence of ultrasonic. Different size specimens were employed to analyze size dependence of acoustic softening effect, and a new material model on basis of surface grain theory was proposed. To explain the mechanism of size dependence of ultrasonic vibration effects, the surface grain flow stress is calculated with surface grain model. Numerical simulations were carried out to validate and compare with experimental results.

2. Experimental Setup

2.1 Ultrasonic vibration-assisted compression system

The ultrasonic vibration-assisted compression (UVAC) system contains an ultrasonic generator (USG-30), a load transducer, a signal amplifier and a data recorder (OMRON ZR-RX 70). Fig. 1 shows the ultrasonic vibration-assisted compression device and schematic of the system. In this study, to meet the requirement of miniaturization, much

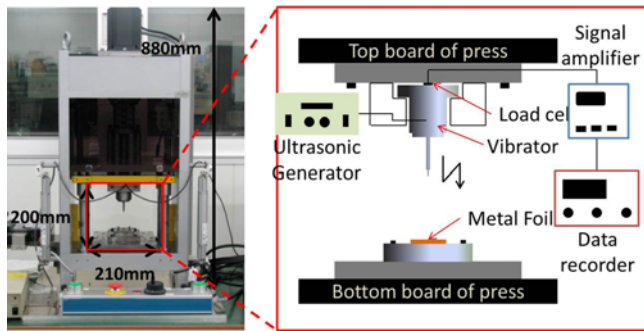


Fig. 1 Ultrasonic vibration-assisted compression system

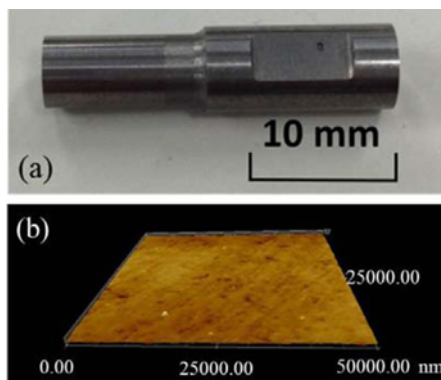


Fig. 2 (a) Punches used for UVAC (b) AFM photograph of punch surface

higher ultrasonic frequency (100 kHz) was used. A problem aroused from high frequency is the vibration amplitude is very small. The maximum vibration amplitude is only 2 μm , far smaller than that of other researchers used.⁸ The UVAC system is fixed on a precision desk top servo press system (DT-J312, Bisai-Kako Inc). The motion resolution of the top board in vertical direction is 1 μm . The punch used for surface finishing is made of tungsten-carbide alloy and has a diameter of 5 mm (Fig. 2(a)). Fig. 2(b) shows the surface image of the punch. The contact surface of the punch is quite smooth, with Ra surface roughness of 12 nm. The punch edge was reserved. The load transducer used in UVAC is LCSH30KN (Output 30 kN) and is provided by Nippon Tokushu Sokki co., Ltd. It is locating on the top board of press machine (Fig. 1). Ra surface roughness was measured with Atomic Force Microscope (KEYENCE Nanoscale Hybrid Microscope VN-8010).

The procedures of operating UVAC system are as follows: 1. Start ultrasonic generator, tune the ultrasonic generator to find the proper inherent frequency to obtain maximum amplitude. 2. Use a cover plate to fix the specimen on die. 3. Move the top board of press machine to proper position to find contact point manually. 4. Activate press machine to move downward at certain speed. 5. Stop ultrasonic vibration, and lift up top board of press machine. 6. Take off the specimens for next analysis. A “contact point” should be marked to define at what height the punch starts to press the sample. Here the load of 5 N is regarded as the “contact load”. When the load reading is 5 N, the position of punch is treated as the contact point.

Table 1 Mechanical properties of brass C3604¹¹

Young's Modulus E / [GPa]	Tensile strength σ_b / [MPa]	Yield strength $\sigma_{0.2}$ / [MPa]	Hardness HB
100	630	500	140

Table 2 Dimension and loading conditions of specimens used for UVAC

Group number	1	2	3	4	5
Diameter [mm]	0.51	0.71	1.0	1.4	1.96
Height [mm]	0.51	0.71	1.0	1.4	1.96
Strain rate [s^{-1}]	0.02	0.02	0.02	0.02	0.02
Loading speed [mm/s]	0.01	0.014	0.02	0.028	0.0392

2.2 Materials and experiment conditions

The material used in this compression test is brass C3604, and its mechanical properties are presented in Table 1. The brass bar was machined into cylinder specimens with different dimensions, and polished to get a smooth surface. To minimize the influence of work hardening of specimens during machining process, all specimens were annealed at 300°C for 30 min. The processed sample has grain size of 19 μm .⁹

The ultrasonic vibration amplitude is set to 1.2 μm . The height reduction of all specimens is 40% (true strain of 0.51). According to the similarity of metal forming, the loading speed should also be determined on basis of specimen size.¹⁰ The ratio of characteristic length of the nearby two groups of specimen is 1.4. The dimensions of specimens and loading speed for each size of specimen are presented in Table 2. To eliminate influence of friction, powder graphite (FC-169) was used as the lubricant.

3. Experimental Results and Discussions

Influence of ultrasonic vibration on brass deformation behavior is mainly discussed in three aspects: flow stress, friction and heat effect. Numerical simulations were carried out to validate and compare with experiment results.

3.1 Influence of ultrasonic on flow stress

The flow stress curves of different specimens compressed with and without ultrasonic vibration are shown in Fig. 3. From this figure, it is found that without presence of ultrasonic vibration, the yield points and material flow stresses are decreasing with the dimension of specimens downscaling. The yield stress of material decreases from 501 MPa at diameter of 1.96 mm to 374 MPa when diameter is 0.51 mm. This typical size effect phenomenon in metal forming has been investigated by many researchers.¹²⁻¹⁴ It is also found that the flow stress in plastic deformation stage of specimen compressed with ultrasonic is lower than that without ultrasonic, which could attribute to acoustic softening effect of ultrasonic on the material. What is interesting is the difference between flow stresses with and without ultrasonic is not constant when the specimen dimension is changing. For the smaller sample, the difference is larger, for the larger diameter sample, the difference becomes smaller.

Fig. 4(a) shows the average flow stress reduction caused by

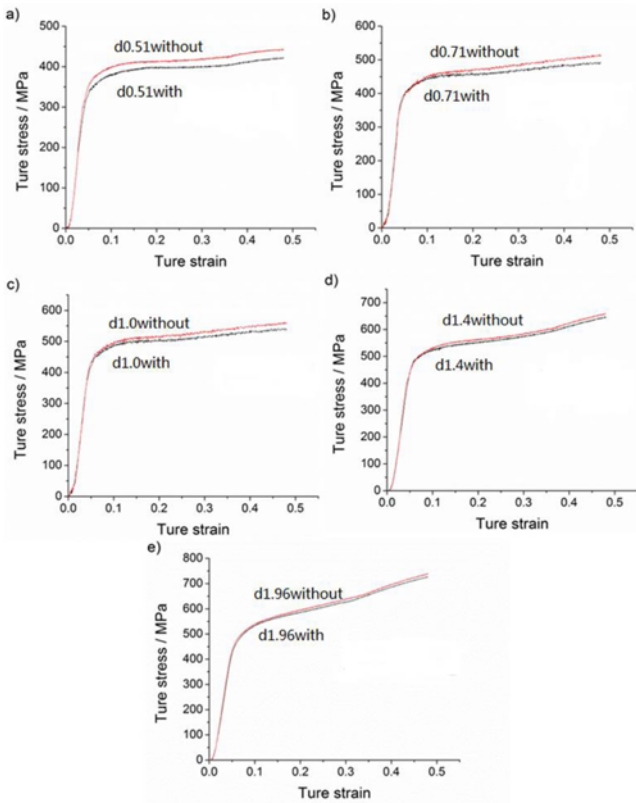


Fig. 3 Flow stress curves of different specimens with and without ultrasonic vibration

ultrasonic in plastic deformation stage. The ultrasonic-induced flow stress reduction is merely 1.25% at diameter of 1.96 mm, while this value increases to 4.7% at 0.51 mm. This suggests that the softening effect of ultrasonic is getting larger when the size of specimen getting smaller, in other word, the acoustic softening effect is size dependent. Up to now, some researchers have concluded that the acoustic softening effect of ultrasonic could contribute to the increase of dislocation motion ability due to absorbing ultrasonic energy,¹⁵ and the ultrasonic softening effect has been validated by experimental or simulation method,^{16,17} but no reference about its size dependence could be found. In this study, a new model developed from surface grain theory was proposed to investigate size-dependent ultrasonic softening effect.

Previous studies^{18,19} suggest that the dislocations absorb much ultrasonic energy and the mobility and rearrangement of dislocation could be greatly increased. It is well known that the material flow stress has a close relation with dislocation density: in normal metal material, with higher dislocation density, the dislocation motion is more difficult, and the material could endure higher stress, the flow stress will be higher. As the mobility of dislocation increases, more dislocations could annihilate on the surface of samples, which results in less dislocation tangling and lower dislocation density in surface layer grains, and this makes the surface layer easier to deform compared with inner grains.

Based on the surface grain theory,²⁰ the material flow stress is a compromise of the property of surface layer grains and inner grains. As the surface grains become softer, the property of the whole specimen would be changed. As the specimens size downscaling, the surface /

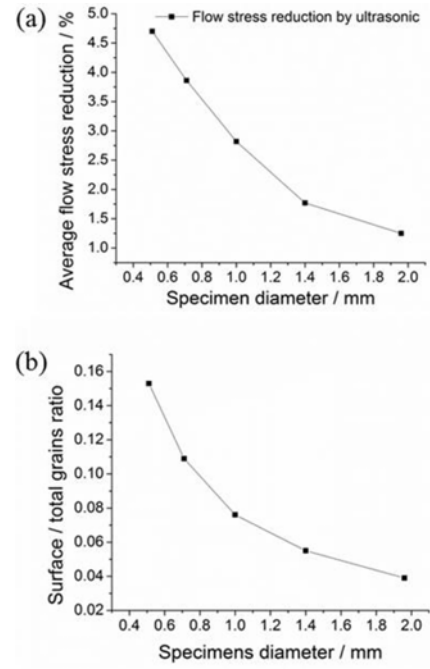


Fig. 4 (a) Average flow stress reduction caused by ultrasonic of different specimens (b) Relationship between specimens diameter and η

total grains ratio η increases, and the ultrasonic softening effect will increase. The flow stress ($\sigma_{ult}(\epsilon)$) obtained from experiment is composite of flow stress of surface grains ($\sigma_{sur}(\epsilon)$) and inner grains ($\sigma_{in}(\epsilon)$), and it could be written as Eq. (1). The surface grain number N_{sur} , total grains number N and surface / total grains ratio η could be expressed as Eqs. (3) (4) and (5).

$$\sigma_{ult}(\epsilon) = \eta \cdot \sigma_{sur}(\epsilon) + (1 - \eta) \cdot \sigma_{in}(\epsilon) \quad (1)$$

$$\sigma_{sur}(\epsilon) = (1/\eta) \cdot [\sigma_{ult}(\epsilon) - (1 - \eta) \cdot \sigma_{in}(\epsilon)] \quad (2)$$

$$N_{sur} = S/S_a - 2\pi D/d = (\pi D \cdot H + 0.5\pi D^2)/(0.25\pi d^2) - 2\pi D/d \quad (3)$$

$$N = (\pi D^2 \cdot H)/(4d^3) \quad (4)$$

$$\eta = N_{sur}/N \quad (5)$$

where D is specimen diameter, H is specimen height, d is grains diameter.

The relationship between specimens diameter and η is shown in Fig. 4(b). The surface / total grains ratio increases from 3.9% at diameter of 1.96 mm to 15.3% at 0.51 mm. It is found the surface / total grains ratio has same trend with average flow stress reduction as shown in Fig. 4(a).

At same vibration amplitude and frequency, influence of ultrasonic softening effect on surface grains will be the same regardless what the sample diameter is. To investigate the softening effect of ultrasonic on surface grains, for different specimen size, the flow stress obtained without ultrasonic was regarded as $\sigma_{in}(\epsilon)$. The flow stress curve obtained from experiment with ultrasonic was used as $\sigma_{ult}(\epsilon)$. So the flow stress reduction caused by size effect has been eliminated, the only acting factor leading to lower flow stress is ultrasonic softening effect on surface grains. In the discussion of size effect using surface grains

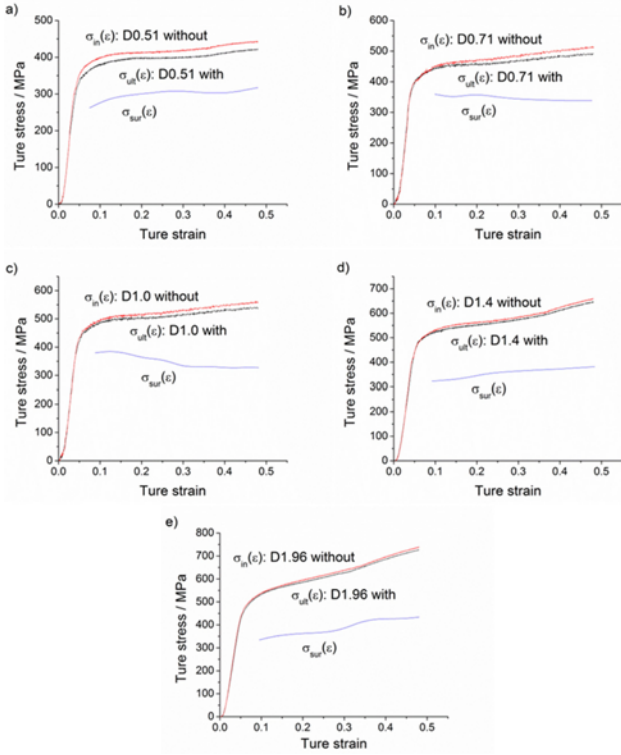


Fig. 5 $\sigma_{in}(\epsilon)$, $\sigma_m(\epsilon)$ and $\sigma_{sur}(\epsilon)$ of different specimens

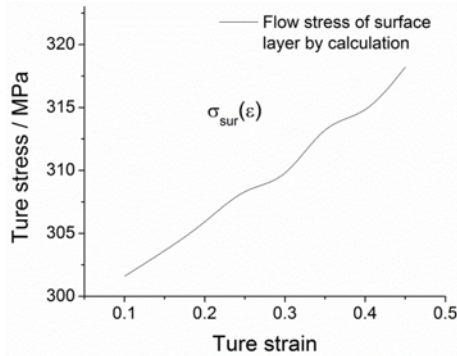


Fig. 6 Average $\sigma_{sur}(\epsilon)$ of different size specimens

model, Peng²¹ treated the surface grains as single crystal and used critical shear resolved stress of the single crystal to represent $\sigma_{sur}(\epsilon)$. However, the stress state of surface grains with ultrasonic would be different from the single crystal, which means the same representation is not appropriate in this case. In this study, $\sigma_{sur}(\epsilon)$ could be calculated with Eq. (2) based on η , $\sigma_{in}(\epsilon)$ and $\sigma_m(\epsilon)$. $\sigma_{in}(\epsilon)$, $\sigma_m(\epsilon)$ and $\sigma_{sur}(\epsilon)$ of different specimens are presented in Fig. 5. The elastic stage is ignored here. $\sigma_{sur}(\epsilon)$ maintains in the range of 260~360 MPa for different specimen sizes. The average value of $\sigma_{sur}(\epsilon)$ of different size specimens (shown in Fig. 6) could be regarded as the real flow stress of the surface grains at ultrasonic amplitude of 1.2 μm and frequency of 100 kHz. Based on Fig. 6, the flow stress of surface grains was found much lower than inner grains due to the combined influences of size effect and ultrasonic softening effect. The calculation results of strain – stress curve of surface grains $\sigma_{sur}(\epsilon)$ (shown in Fig. 6) validates that due to

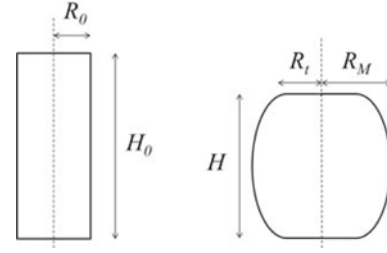


Fig. 7 A simple model of compression test

the surface grains are softer than inner grains, lower flow stress could be attributed to larger share of surface grain in smaller sample.

3.2 Influence of ultrasonic on friction

Since the ultrasonic vibration-assisted compression is a dynamic process, the pressure between punch surface and specimen is not constant, the frictional condition is different from the static one. The friction coefficient was evaluated to see influence of ultrasonic vibration with different amplitudes on friction in compression test. Ultrasonic amplitude was set to 0, 0.8 μm , 1.2 μm and 1.6 μm . Only specimen of diameter 1.0 mm was used and no lubricant was employed.

The friction coefficient between tools and samples could be determined in various methods. The most common way is using compression ring test.²² Strip drawing is another way to measure friction.²³ However, both of these methods are not suitable for ultrasonic-assisted compression, due to the specimen dimension is too small to handle. R. Ebrahimi and A. Najazadeh²⁴ proposed a new method to evaluate friction in bulk deformation which is on basis of upper-bound theory. It is especially suitable for small specimen friction measurement because the geometrical shape could be obtained precisely with microscope. This method was employed to obtain friction in this study.

A simplified model of compression test is shown in Fig. 7. The cylinder specimen will bulge due to the friction. If the friction coefficient is large, RM (shown in Fig. 7) will be larger. Based on R. Ebrahimi's method, the friction coefficient could be calculated with Eq. (6).

$$m = \left[\left(\frac{R}{H} \right) b \right] \left(\frac{4}{\sqrt{3}} - \frac{2b}{3\sqrt{3}} \right) \quad (6)$$

where m is the average friction coefficient, with its value ranging from 0 (perfect sliding) to 1 (sticking friction); b is the barreling factor; and R and H are the theoretical radius and initial height of the sample, respectively. b could be written as Eq. (7). ΔR is the difference between the maximum radius R_M and the radius R_t of top surface of the sample, and ΔH is the reduction in the height of the cylinder after compression.

$$b = 4(\Delta R/R) \cdot (H/\Delta H) \quad (7)$$

$$R = R_0 \sqrt{H_0/H} \quad (8)$$

$$\Delta R = R_M - R_t \quad (9)$$

$$\Delta H = H_0 - H \quad (10)$$

The relevant parameters in Eq. (6) could be obtained from the SEM photographs as shown in Fig. 8. The frictional coefficients calculated

Table 3 Friction coefficient calculated from Eq. (6)

Amplitude [μm]	0	0.8	1.2	1.6	bottom
m	0.44122	0.27944	0.01418	0.08732	0.55887

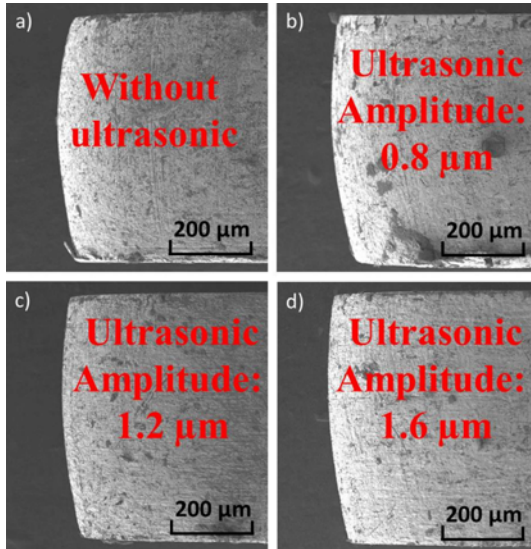


Fig. 8 SEM photographs of specimens compressed with ultrasonic

with Eq. (6) are listed in Table 3.

“Bottom” in Table 3 means the friction between sample and die surface. In this study, the die surface is much rougher than punch, as a result, the friction coefficient between die is higher than between punch. The figure shows that ultrasonic vibration has little influence on the friction between sample and die. From Table 3, it is found that if no ultrasonic vibration is applied (amplitude = 0), the friction coefficient between die and sample is about 0.44. With presence of ultrasonic, the friction coefficient becomes much lower. Even amplitude is very low, for example 0.8 μm , the coefficient decreases to 0.28, with a reduction of 35.4%. Keep on increasing amplitude, the friction coefficient reduces to 0.14 at amplitude of 1.2 μm , and 0.087 at 1.6 μm .

FEM simulation was used to estimate the friction coefficients at the interfaces to compare with the calculated values from the above analysis. Abaqus v 6.12.1 was used for the simulation. The punch and die was modeled as rigid body, while specimen was modeled as a two dimensional plane deformable body. The flow stress curves of brass obtained in experiment was input as property of the material. Die kept unmoved through the process and punch moved downwards at a constant speed of 0.02 mm/s. Apply the friction coefficient obtained from the analytical model (0.08 for vibrated top surface, 0.44 for unvibrated top surface, 0.55 for bottom surface), and compare the samples profiles with the samples deformed in experiment. Fig. 9 presents the comparison of results of simulation and experiment. The results state that the when the top friction coefficient is 0.08, and bottom friction coefficient is 0.55, the profile of the deformed cylinder matches the SEM photograph very well (Fig. 9(d)). This indicates the friction coefficient between sample top surface and punch decreases to 0.08 from 0.44 under the influence of ultrasonic.

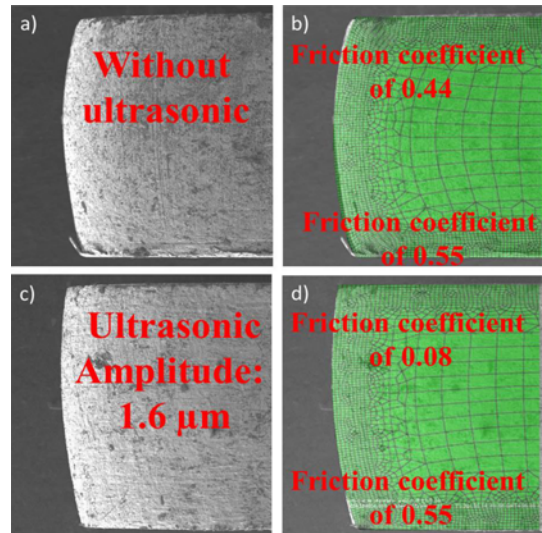


Fig. 9 Comparison of results of simulation and experiment

3.3 Influence of ultrasonic on specimen temperature

During the ultrasonic vibration assisted compression test, the metal material vibrates at very high frequency, which will produce additional heat, and the temperature of specimen will increase. Using a thermal couple (KFC-50-200-050), the temperature of samples deformed with and without vibration could be obtained. Even the contact surfaces with die and punch have higher temperature, the heat distribution will get uniform in the whole samples due to the dimensions are all very small and high heat conductivity of metal. In this case, for simplicity of operation, one point on the side surface of the middle part of specimen is selected to measured temperature, and this value is used to represent the temperature of the whole sample. Fig. 10 shows the results of temperature measurement of diameter 1.0 mm specimens under ultrasonic amplitude of 0.8 μm , 1.2 μm and 1.6 μm . Due to higher energy input, the sample deformed at higher amplitude has higher temperature. But the temperature increase is very low. Even deformed at ultrasonic of 1.6 μm amplitude, the temperature increase from room temperature (25°C) is merely 12°C. Fig. 11 is the temperature of different diameter specimens compressed at ultrasonic with amplitude of 1.2 μm . It is found that the smaller sample has lower temperature, which could attribute to that the heat produced from surface friction is smaller. Similarly, the increase from room temperature is also very low, less than 20°C. Based on the temperature measurement, it is found that ultrasonic is able to increase the specimen temperature, but the temperature increase is very low. This could ascribe to small amplitude of ultrasonic and the high heat conductivity between punch and sample. Other researcher reported the heat effect of ultrasonic, and the temperature increase is also very low.²⁵ This indicates the influence of heat effect of ultrasonic on plastic deformation behavior of material is hardly detectable, which could be neglected.

4. Conclusions

In this study, the ultrasonic vibration-assisted compression test was carried out and influences of ultrasonic were surveyed in detail. FEM

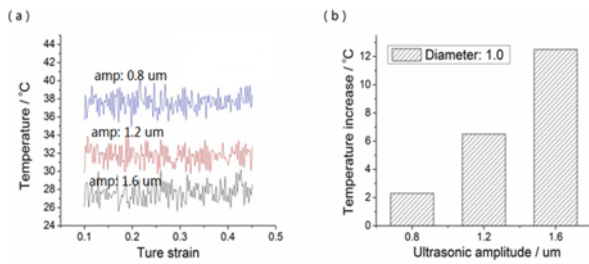


Fig. 10 (a) Temperature of diameter 1.0 specimen with ultrasonic of different amplitudes (b) average increase from room temperature (25°C)

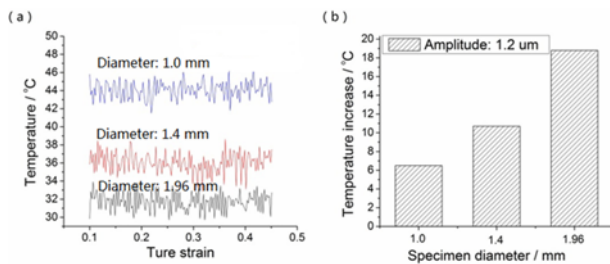


Fig. 11 (a) Temperature of specimens with different diameter with same ultrasonic (b) average increase from room temperature (25°C)

simulation of UVAC was conducted to validate and compare with experimental results. Based on the results, the following conclusions could be drawn:

1. The material flow stress decreases with samples size. The decrease of flow stress has similar trend with surface / total grains ratio.
2. At influence of ultrasonic and size effect, the flow stress of surface grains is much lower than inner grains.
3. Ultrasonic vibration has a softening effect on brass flow stress, and this effect could be explained from the view of dislocation mobility in surface grain under ultrasonic influence.
4. With presence of ultrasonic vibration, the friction coefficient is reduced. Higher ultrasonic amplitude yields lower frictional coefficient. The calculated frictional coefficient with the analytical model agrees with simulation well.
5. Ultrasonic heat effect was detected, but the temperature increase is so low that could not generate visible influence on deformation behavior of brass.

ACKNOWLEDGEMENT

The authors acknowledge the financial support by National Natural Science Foundation of China through grant no. 51405296.

REFERENCES

1. Blaha, F. and Langenecker, B., "Elongation of Zinc Monocrystals under Ultrasonic Action," *Die Naturwissenschaften*, Vol. 42, No. 20, p. 556, 1955.
2. Langenecker, B., "Effects of Ultrasound on Deformation Characteristics of Metals," *IEEE Transactions on Sonics and Ultrasonics*, Vol. 13, pp. 1-8, 1966.
3. Huang, H., Pequegnat, A., Chang, B., Mayer, M., Du, D., and Zhou, Y., "Influence of Superimposed Ultrasound on Deformability of Cu," *Journal of Applied Physics*, Vol. 106, No. 11, Paper No. 113514, 2009.
4. Abdul Aziz, S. and Lucas, M., "The Effect of Ultrasonic Excitation in Metal Forming Tests," *Applied Mechanics and Materials*, Vols. 24-25, pp. 311-316, 2010.
5. Yao, Z., Kim, G. Y., Faidley, L., Zou, Q., Mei, D., and Chen, Z., "Effects of Superimposed High-Frequency Vibration on Deformation of Aluminum in Micro/Meso-Scale Upsetting," *Journal of Materials Processing Technology*, Vol. 212, No. 3, pp. 640-646, 2012.
6. Huang, H., Pequegnat, A., Chang, B., Mayer, M., Du, D., and Zhou, Y., "Influence of Superimposed Ultrasound on Deformability of Cu," *Journal of Applied Physics*, Vol. 106, No. 11, Paper No. 113514, 2009.
7. Hung, J. C. and Hung, C., "The Influence of Ultrasonic-Vibration on Hot Upsetting of Aluminum Alloy," *Ultrasonics*, Vol. 43, No. 8, pp. 692-698, 2005.
8. Wang, T., Wang, D. P., Liu, G., Gong, B., Song, N. X., "Investigations on the Nanocrystallization of 40Cr using Ultrasonic Surface Rolling Processing," *Applied Surface Science*, Vol. 255, No. 5, pp. 1824-1829, 2008.
9. Kosuge, S., "Effects of Ultrasonic Vibration on Transfer Property," M.Sc. Thesis, Department of System Design, Tokyo Metropolitan University, 2013.
10. Zhang, K. F. and Kun, L., "Classification of Size Effects and Similarity Evaluating Method in Micro Forming," *Journal of Materials Processing Technology*, Vol. 209, No. 11, pp. 4949-4953, 2009.
11. Huang, B. Y., Li, C. G., Shi, L. K., Qiu, G. Z., and Shi, T. Y., "China Materials Engineering Canon," Chemical Industry Press, pp. 264-266, 2005.
12. Michel, J. F. and Picart, P., "Size Effects on the Constitutive Behaviour for Brass in Sheet Metal Forming," *Journal of Materials Processing Technology*, Vol. 141, No. 3, pp. 439-446, 2003.
13. Gau, J. T., Principe, C., and Wang, J., "An Experimental Study on Size Effects on Flow Stress and Formability of Aluminum and Brass for Microforming," *Journal of Materials Processing Technology*, Vol. 184, No. 1, pp. 42-46, 2007.
14. Kals, T. A., and Eckstein, R., "Miniaturization in Sheet Metal Working," *Journal of Materials Processing Technology*, Vol. 103, No. 1, pp. 95-101, 2000.
15. Savkina, R. K. and Smirnov, A. B., "Temperature Rise in Crystals Subjected to Ultrasonic Influence," *Infrared Physics & Technology*, Vol. 46, No. 5, pp. 388-393, 2005.

16. Siddiq, A. and El Sayed, T., "Acoustic Softening in Metals during Ultrasonic Assisted Deformation Via CP-FEM," *Materials Letters*, Vol. 65, No. 2, pp. 356-359, 2011.
17. Siddiq, A. and Ghassemieh, E., "Thermomechanical Analyses of Ultrasonic Welding Process using Thermal and Acoustic Softening Effects," *Mechanics of Materials*, Vol. 40, No. 12, pp. 982-1000, 2008.
18. Hirao, M., Ogi, H., Suzuki, N., and Ohtani, T., "Ultrasonic Attenuation Peak during Fatigue of Polycrystalline Copper," *Acta Materialia*, Vol. 48, No. 2, pp. 517-524, 2000.
19. Min, X. and Kato, H., "Change in Ultrasonic Parameters with Loading/Unloading Process in Cyclic Loading of Aluminium Alloy," *Materials Science and Engineering: A*, Vol. 372, No. 1, pp. 269-277, 2004.
20. Engel, U. and Eckstein, R., "Microforming-from Basic Research to Its Realization," *Journal of Materials Processing Technology*, Vol. 125, No. pp. 35-44, 2002.
21. Peng, L., Lai, X., Lee, H. J., Song, J. H., and Ni, J., "Analysis of Micro/Mesoscale Sheet Forming Process with Uniform Size Dependent Material Constitutive Model," *Materials Science and Engineering: A*, Vol. 526, No. 1, pp. 93-99, 2009.
22. Wang, J. P., "A New Evaluation to Friction Analysis for the Ring Test," *International Journal of Machine Tools and Manufacture*, Vol. 41, No. 3, pp. 311-324, 2001.
23. Shimizu, T., Manabe, K., and Yang, M., "Deformation Behavior of Ultra-Thin Metal Foils in Strip Drawing Friction Test," *Key Engineering Materials*, Vol. 443, pp. 110-115, 2010.
24. Ebrahimi, R. and Najafzadeh, A., "A New Method for Evaluation of Friction in Bulk Metal Forming," *Journal of Materials Processing Technology*, Vol. 152, No. 2, pp. 136-143, 2004.
25. Hung, J. C. and Lin, C. C., "Investigations on the Material Property Changes of Ultrasonic-Vibration Assisted Aluminum Alloy Upsetting," *Materials & Design*, Vol. 45, pp. 412-420, 2013.